Quantum Electronics **38** (9) 884 – 888 (2008)

LASER COOLING

PACS numbers: 37.10.De; 37.10.Gh
DOI: 10.1070/QE2008v038n09ABEH013687

Measurement of the lifetime of rubidium atoms in a dark magneto-optical trap

O.I. Permyakova, A.V. Yakovlev, P.L. Chapovsky

***Abstract*. The lifetimes of rubidium atoms in a dark magneto-optical trap are measured at different populations of the 'bright' and 'dark' hyperfine states of captured atoms. It is found that the lifetime of atoms in the trap decreases if they spend more time in the bright state. A simple explanation of this effect is proposed which is based on the increase in the transport cross section for collisions of thermal rubidium atoms surrounding the trap with cold rubidium atoms upon their electronic excitation.**

Keywords: *laser cooling of rubidium, dark magneto-optical traps.*

1. Introduction

Laser cooling of neutral atoms in magneto-optical traps (MOTs) is an important tool of modern atomic physics [1, 2]. These traps are convenient and reliable devices for cooling a great number of atoms down to temperatures of $10 - 10^2$ μK. Magneto-optical traps are used in the laser spectroscopy of cold atoms, investigations of atomic collisions at low temperatures, in the development of new frequency standards, at the initial cooling stage for producing the Bose – Einstein condensation of rarefied gases, and in other fields.

The direct use of MOTs for spectroscopic studies of cold atoms is complicated because the laser and magnetic fields of the trap produce strong perturbations of the electronic structure of trapped atoms. This problem can be solved by separating in time the capture of atoms in the trap and spectroscopic studies of cold atoms. A disadvantage of this method is that in this case we are dealing with a nonstationary object – the expanding cloud of atoms released from the trap.

The difficulties can be eliminated in a number of cases by using a modified MOT – the so-called dark MOT (DMOT), which was proposed in [3] for alkali metal atoms. A dark MOT consists of two spatial regions. The external region of the trap contains cooling and repumping (returning atoms on the levels interacting with cooling radiation) laser radiations and operates as a usual MOT. In the internal region, repumping radiation is absent, and therefore atoms are accumulated here in the 'dark' hyperfine state and do not interact with cooling radiation. However, due to the scattering of repumping radiation by optical elements of the system and thermal atoms of the cooled gas, this radiation penetrates nevertheless into the internal region of the DMOT. As a result, a fraction of trapped atoms populates the 'bright' hyperfine state and interacts with cooling radiation. Note that it is atoms in the bright state that produce fluorescence of the atomic cloud in the DMOT.

The main applications of DMOTs are based on their ability to increase considerably the density and number of captured atoms. This is explained by the fact that the repulsion of particles due to radiation exchange between atoms and hyperelastic collisions are suppressed in DMOTs. (Recall that during hyperelastic collisions, the internal energy of excited atoms is transformed to the kinetic energy.) Along with this useful property (to hold a greater part of trapped atoms in the dark state), the populations of the bright and dark states in a DMOT can be varied in a broad range. The populations of these states determine a number of physical processes in the DMOT, for example, the absorption of laser radiation by cold atoms. Thus, a change in the fraction of atoms in the bright hyperfine state can be used for studying the physics of cold atoms. In this paper, we studied experimentally the dependence of the lifetime of rubidium atoms in a dark trap on the relative populations of the bright and dark states.

2. Energy level diagram of rubidium atoms and a DMOT

We performed experiments with ^{85}Rb atoms. The energy level diagram of these atoms is presented in Fig. 1. We used two DL100 lasers (Toptica) to form a trap. The cooling radiation frequency ν_{col} is shifted to the red by 15 – 20 MHz from the central frequency of the $F_g = 3 \rightarrow F_e = 4$ transition. The repumping radiation frequency ν_{rep} was varied in a broad range in the region of frequencies ν_{22} and ν_{23} of the $F_g = 2 \rightarrow F_e = 2, 3$ transitions, respectively (see below). The hyperfine states with $F_g = 2$ and 3 are the dark and bright states, respectively.

The scheme of the experimental setup is shown in Fig. 2a. Our DMOT captures atoms directly from the gas of thermal rubidium atoms in a vacuum chamber (similarly to the approach proposed in [2] for a usual MOT). The trap is formed by six circularly polarised cooling beams and two linearly polarised repumping beams. The

O.I. Permyakova, A.V. Yakovlev, P.L. Chapovsky Institute of Automation and Electrometry, Siberian Branch, Russian Academy of Sciences, prosp. Akad. Koptyuga 1, 630090 Russia;
e-mail: chapovsky@iae.nsk.ru

Received 12 July 2007; revision received 5 May 2008
Kvantovaya Elektronika **38** (9) 884 – 888 (2008)
Translated by M.N. Sapozhnikov

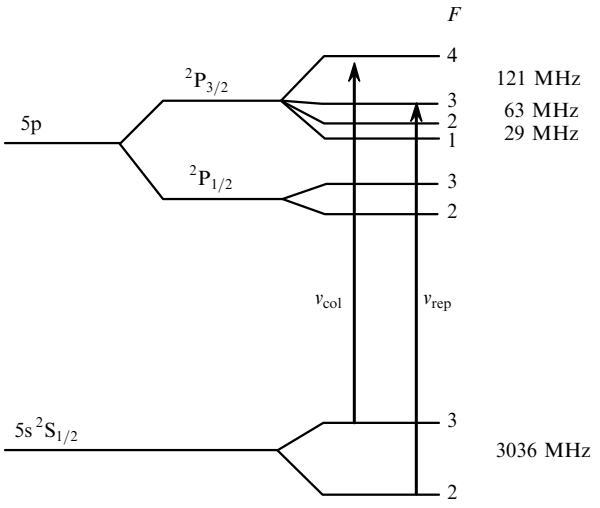

Figure 1. Energy level diagram of ^{85}Rb: F is the angular momentum of the hyperfine state; hyperfine splittings are indicated on the right.

power of each of the beams is 6 mW and diameter is $\sim$ 15 mm. Two 'hollow' repumping beams are directed to the centre of the trap at an angle of 90° to each other (the intensity distribution in the cross section of these beams is a circle with the internal and external diameters 5 and 15 mm, respectively).

The magnetic field of a quadrupole configuration was produced by two 'anti-Helmholtz' coils (100 turns, diameter 5 cm) separated by a distance of 5 cm. The current in the coils equal to 1.6 A produced a magnetic field at the trap centre with a gradient of 17 G cm^{-1} along the symmetry axis of the system. The magnetic field could be switched on (and switched off) for the time shorter than 500 μs.

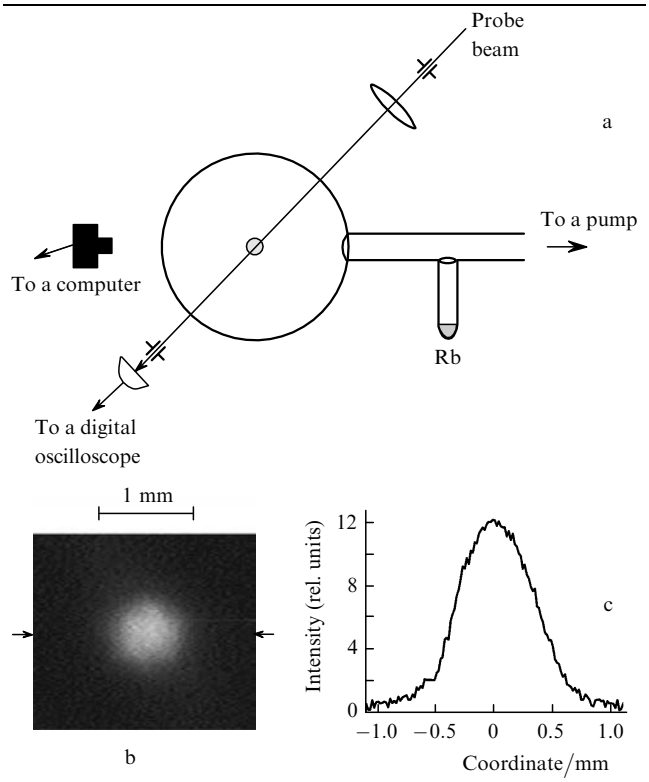

Figure 2. Scheme for measuring the amount of rubidium atoms captured in the DMOT (Helmholtz coils and cooling and repumping radiation beams are not shown) (a), the spatial distribution of the fluorescence intensity of the cloud of cold rubidium atoms in the DMOT (b), and the cross section of this distribution along the direction indicated by the arrows (c).

We used a simple vacuum chamber for the DMOT, which was a glass sphere of diameter 6 cm without an additional AR coating. The chamber was permanently connected with an ion pump (of capacity $\sim$ 10 L s^{-1}) with a glass side arm containing metal rubidium. The pressure of rubidium vapour in the chamber was controlled by cooling this side arm with a Peltier element. Because the trap chamber was permanently evacuated by the pump, the rubidium vapour pressure was considerably lower than the saturated vapour pressure corresponding to the side arm temperature. The pressure of residual gases (rubidium vapour and, probably, helium and hydrogen) in the chamber did not exceed 10^{-8} Torr. Additional information on the MOT and parameters of captured atoms is presented in [4–6].

Populations of the hyperfine levels of the ground electronic state of rubidium were measured by the absorption of a probe beam from an additional semiconductor laser. This laser (Mitsubishi ML6XX24 diode) operated without the external cavity and had a highly stable current supply and a precision thermal stabilisation system. The linewidth (HWHM) of the probe laser was, according to our estimate, smaller than 1 MHz.

All the three lasers used in our experiments had frequency-stabilisation systems based on the DAVLL (dichroic atomic vapour laser lock) method [7, 8]. These systems provided the laser frequency stabilisation with a drift of less than 3 MHz h^{-1} at any point of a broad ($\sim$ 1 GHz) frequency range near the frequency of each hyperfine absorption line of Rb. Additional information on our laser frequency stabilisation system is presented in paper [9].

3. Experimental results

The stationary amount of captured rubidium atoms depends on the concentration of thermal rubidium atoms in the vacuum chamber. If the side arm containing metal rubidium has room temperature, the total number of captured rubidium atoms in our dark trap achieves $\sim 10^8$. The cloud of atoms has almost spherical shape of diameter 0.8 mm (Fig. 2b). The shape of the cloud was determined from the spatial distribution of the fluorescence intensity recorded with an analogue video camera. The output signal of the video camera was digitised and analysed by using the Mathcad packet.

Figure 3 presents the results of measuring the amount of rubidium atoms captured in the DMOT at different repumping radiation frequencies. These data were obtained at the room temperature of the side arm. The repumping radiation frequency was measured by using saturated absorption resonances in counterpropagating fields in an additional cell with rubidium vapour of length 7 cm at room temperature. These resonances for the $F_g = 2 \rightarrow F_e = 1, 2, 3$ hyperfine transitions are shown in Fig. 3a. Because the linear absorption spectrum has three allowed transitions, the saturated absorption spectrum consists of six peaks. The frequency scale of this spectrum was determined from resonance frequencies measured in [10]. For convenience,

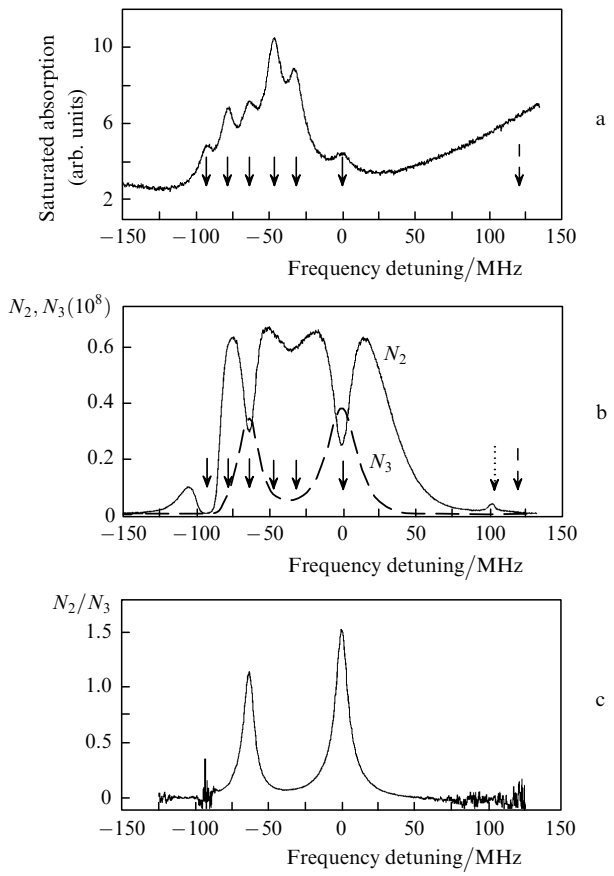

Figure 3. Saturated absorption resonances at the $F_g = 2 \rightarrow F_e = 1, 2, 3$ transitions (a), the amount of atoms N_2 and N_3 in the $F_g = 2$ and 3 states, respectively (b), and the ratio N_3/N_2 (c). The solid arrows show the positions of saturated resonances (see Table 1), the dashed arrows show the central frequency of the forbidden $F_g = 2 \rightarrow F_e = 4$ transition, the dotted arrow shows the position of the combination resonance for cooling and repumping radiations. The zero frequency detuning corresponds to the central frequency of the $F_g = 2 \rightarrow F_e = 3$ transition.

the frequencies of saturated absorption resonances are presented in Table 1 (double transitions indicate cross resonances).

Figure 3b presents the dependences of the amount N_2 and N_1 of rubidium atoms in the $F_g = 2$ and 3 states, respectively, on the repumping radiation frequency. These data were obtained by slowly scanning the repumping radiation frequency to take into account a long filling time of the trap (see below). The amount of captured rubidium atoms in the $F_g = 2$ state was measured by tuning the probe radiation frequency to the central frequency of the $F_g = 2 \rightarrow F_e = 1$ transition. This transition is most suitable for measuring the concentration of atoms in the $F_g = 2$ state because it is closed and, therefore, is subjected to field saturation to a lesser degree than two other allowed transitions beginning from the same hyperfine level. The amount of captured atoms in the $F_g = 3$ state was measured by the absorption of probe radiation at the $F_g = 3 \rightarrow F_e = 2$ transition. This transition is the least perturbed by the cooling radiation. The absorption spectra of probe radiation were then compared with the calculated absorption spectrum of a weak field and, finally, taking the cloud volume into account (Fig. 2b), gave the total amount of captured atoms in the $F_g = 2$ and 3 states. The accuracy of measuring N_2 and N_3 was $\sim 20\%$.

Table 1. Frequencies of saturated absorption resonances in ^{85}Rb vapour for transitions beginning from the $F_g = 2$ hyperfine state [10].

$F_g \rightarrow F_e$ transition	Frequency detuning/MHz
$2 \rightarrow 1$	−92.82
$2 \rightarrow 1, 2 \rightarrow 2$	−78.11
$2 \rightarrow 2$	−63.4
$2 \rightarrow 1, 2 \rightarrow 3$	−46.41
$2 \rightarrow 2, 2 \rightarrow 3$	−31.7
$2 \rightarrow 3$	0

The frequency dependence of N_3 (Fig. 3b) has two maxima at the frequencies coinciding with ν_{22} and ν_{23}. The frequency dependence of N_2 is more complicated. This dependence exhibits two broad maxima and two narrow minima at frequencies ν_{22} and ν_{23}. The maxima in the frequency dependences of N_2 and N_3 are caused by the increase in the efficiency of transfer of atoms from the $F_g = 2$ level to the $F_g = 3$ level by repumping radiation in the external region of the DMOT, when the frequency of this radiation becomes close to the frequencies of the unclosed $F_g = 2 \rightarrow F_e = 2, 3$ transitions. These maxima have a broad spectral width due to the large 'field broadening'. The narrow minima in the frequency dependence of N_2 are related to the transition of cold rubidium atoms from the hyperfine $F_g = 2$ level to the hyperfine $F_g = 3$ level in the internal region of the DMOT, which is caused by weak scattered repumping radiation. The widths of the narrow holes are close to the radiative widths of the $F_g = 2 \rightarrow F_e = 2, 3$ transitions, which confirms the low intensity of radiation involved in this process. Additional information on the spectral parameters of rubidium atoms in the DMOT are presented in paper [6].

Consider now the dependence of the ratio N_3/N_2 on the repumping radiation frequency (Fig. 3c). This dependence has two maxima at frequencies ν_{22} and ν_{23} and a deep minimum at the repumping radiation frequency ν_{mid} lying between these central frequencies. The frequency ν_{mid} is shifted by ~ 40 MHz to the red from frequency ν_{23}. Note that the DMOT ability to capture atoms remains high and approximately the same at all these frequencies. One can see from Fig. 3c that, as the repumping radiation frequency is varied, the ratio N_3/N_2 changes by 20 times, from 1.5 to 0.08.

This property of our DMOT was used to measure the dependence of the lifetime of rubidium atoms in the trap on their electronic state. For this purpose, we measured the dependence of the amount of captured atoms in the $F_g = 2$ state on the time elapsed after the switching on the quadrupole magnetic field of the trap at the three frequencies of repumping radiation ν_{rep}:

$$\nu_{rep} = \nu_{22}, \quad \nu_{rep} = \nu_{23}, \quad \nu_{rep} = \nu_{mid}. \tag{1}$$

Measurements were performed at the temperature of the side arm with metal rubidium lowered down to $-8\,^{\circ}$C. This considerably reduced the pressure of rubidium vapour in the vacuum chamber of the trap and resulted in the decrease in the number of cold atoms in the cloud by 10–20 times compared to the number of atoms captured at the room temperature of the side arm. The reduction of the number of rubidium atoms in the cloud considerably simplified the experimental situation because the cloud became optically thin and the interaction between cold atoms became insignificant.

Figure 4 presents the time dependences of the number of rubidium atoms in the $F_g = 2$ state captured by the DMOT. Curves (*1*) and (*2*) corresponding to the repumping radiation frequencies $\nu_{rep} = \nu_{22}$ and ν_{23} are almost coincident. Curve (*3*), measured for $\nu_{rep} = \nu_{mid}$, demonstrates a considerably longer lifetime of atoms in the trap. The lifetimes of atoms in the trap were

$$\tau_{22} = 0.72 \pm 0.01 \text{ s}, \ \tau_{23} = 0.74 \pm 0.01 \text{ s}, \qquad \tau_{mid} = 1.03 \pm 0.01 \text{ s}. \tag{2}$$

Here, τ_{22} and τ_{23} correspond to $\nu_{rep} = \nu_{22}$ and ν_{23}, respectively. The time dependences of the trap filling presented in Fig. 4 are exponential with an accuracy to statistical measurement errors.

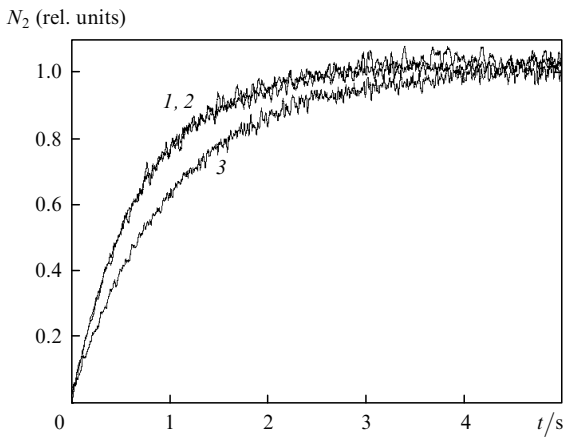

Figure 4. Time dependences of the amount N_2 of rubidium atoms in the F_g state for repumping radiation frequencies $\nu_{rep} = \nu_{22}$ (*1*), ν_{23} (*2*), and ν_{mid} (*3*).

4. Discussion

The lifetime of rubidium atoms in a MOT is determined by a number of physical effects (see, for example, review [11]). The role of some of these effects becomes insignificant at a low density of cold atoms in the cloud used in our experiments for measuring the lifetime of rubidium atoms in the trap. The neglect of the reabsorption of fluorescence of rubidium and hyperelastic collisions in the cloud is justified by the fact that the time dependence of trap filling is purely exponential. In such a simplified situation, atoms in the trap do not interact with each other and the size of the cloud is independent of the number of atoms in it. The number N of cold atoms in the cloud is described by the equation [2]

$$\frac{dN}{dt} = R - \frac{N}{\tau}, \tag{3}$$

where R is the capture rate of rubidium atoms and τ is the lifetime of atoms in the trap. The time τ is determined under our experimental conditions by collisions of cold rubidium atoms with surrounding thermal atoms:

$$\tau^{-1} = n_{Rb}\sigma_{Rb}\upsilon_{Rb} + n_b\sigma_b\upsilon_b, \tag{4}$$

where n_{Rb} and n_b are the concentrations of thermal Rb atoms and atoms of residual gases, respectively, and υ_{Rb} and υ_b are the average thermal velocities of these atoms. The cross sections σ_{Rb} and σ_b characterise collisions after which cold atoms acquire velocities exceeding the critical velocity υ_c (the ejection cross sections). The critical velocity is the maximum velocity of atoms that can be captured in the trap [2]. For our trap, $\upsilon_c \sim 10$ m s^{-1}.

Equation (3) gives the exponential dependence of the number of captured atoms on time with the time constant equal to τ. Thus, by measuring the dynamics of trap filling, we can determine the lifetime of atoms confined in the trap. The difference in the lifetimes of rubidium atoms in the trap observed in experiments at different repumping radiation frequencies can be explained by assuming that the collision cross sections σ_{Rb} and σ_b depend on the electronic state of cold rubidium atoms. The time which a trapped rubidium atom spends in the ground and excited electronic states is considerably different for repumping radiation frequencies ν_{22} (ν_{23}) and ν_{mid} used in our experiments. The results of measurements presented above show that approximately 60% of Rb atoms populate the bright hyperfine state if $\nu_{rep} = \nu_{22}$ or ν_{23}, and only 10 % of these atoms populate this state if $\nu_{rep} = \nu_{mid}$. The rubidium atoms excited to the bight hyperfine state spend approximately half the time in the excited electronic state. Therefore, the fraction of Rb atoms in the $^2P_{3/2}$ state is ~ 30 % if $\nu_{rep} = \nu_{22}$ or ν_{23}, and this fraction is only ~ 5 % if $\nu_{rep} = \nu_{mid}$. By using Eqn (4), we can explain the change in the lifetimes (2) by the change in the amount of Rb atoms in the $^2P_{3/2}$ state if the cross section for ejection of Rb atoms in the $^2P_{3/2}$ state from the trap is three times larger than that for unexcited Rb atoms.

The change in the collision cross section of rubidium atoms upon their electronic excitation was observed earlier in the study of the light-induced drift (LID) of rubidium atoms [12]. The LID value is determined by the difference of transport collision frequencies for excited and unexcited atoms. It was shown in [12] that the change in the transport collision cross section can achieve 50 %. Note that in a usual 'transport' collision, the kinetic energy of the order of the thermal energy k_BT (k_B is the Boltzmann constant) is imparted to an atom

Our measurements give a considerably greater change in the transport collision cross section compared to that observed in LID experiments. However, the process of collision ejection of atoms from the DMOT significantly differs from transport collisions of atoms at room temperature. The ejection of atoms is determined by the cross section for transfer of a rather small kinetic energy ε_{esc} to a cold atom, which is sufficient for the ejection of the atom from the trap. The energy ε_{esc} is two–three orders of magnitude smaller than the thermal energy k_BT at room temperature.

5. Conclusions

We have measured the lifetime of rubidium atoms in the DMOT by varying the ratio of populations of the bright and dark states by 20 times. The measurements have shown that the lifetime of rubidium atoms in the DMOT decreases when the atoms spend more time in the bright state. This effect has been explained by assuming that the cross section for collisions of trapped rubidium atoms in the $^2P_{3/2}$ state with surrounding thermal atoms is larger than that for

rubidium atoms in the ground state. A similar tendency has been observed for the transport collision cross section upon excitation of rubidium atoms in LID experiments [12].

Acknowledgements. This work was supported by the Russian Foundation for Basic Research (Grant Nos 06-02-16415 and 06-02-08134), the Presidium of Siberian Branch, RAS, and the program 'Optical Spectroscopy and Frequency Standards' of the Department of Physical Sciences, RAS.

References

1. Raab E.L., Prentiss M., Cable A., Chu S., Pritchard D.E. *Phys. Rev. Lett.*, **59**, 2631 (1987).
2. Monroe C., Swann W., Robinson H., Wieman C. *Phys. Rev. Lett.*, **65**, 1571 (1990).
3. Ketterle W., Davis K.B., Joffe M.A., Martin A., Pritchard D.E. *Phys. Rev. Lett.*, **70**, 2253 (1993).
4. Chapovsky P.L. *Zh. Eksp. Teor. Fiz.*, **127**, 1035 (2005).
5. Chapovsky P.L. *Kvantovaya Elektron.*, **36**, 257 (2006) [*Quantum Electron.*, **36**, 257 (2006)].
6. Chapovsky P.L. *Zh. Eksp. Teor. Fiz.*, **130**, 820 (2006).
7. Corwin K.L., Lu Z., Hand C.F., Epstein R.J., Wieman C.E. *Appl. Opt.*, **37**, 3295 (1998).
8. Yashchuk V.V., Budker D., Davis J.R. *Rev. Sci. Instrum.*, **71**, 341 (2000).
9. Permyakova O.I., Yakovlev A.V., Chapovsky P.L. *Kvantovaya Elektron.*, **35**, 449 (2005) [*Quantum Electron.*, **35**, 449 (2005)].
10. Barwood G.P., Gill P., Rowley W.R.C. *Appl. Phys. B*, **53**, 142 (1991).
11. Weiner J., Bagnato V.S., Zilio S., Jullenne P.S. *Rev. Mod. Phys.*, **71**, 1 (1999).
12. Wittgrefe F. *Light-Induced Drift of Rubidium and Spectral Properties of Semiconductor Lasers* (Ph.D. Thesis) (Leiden, The Netherlands: Leiden University, 1990).